Optical emission line profiles and X-ray properties of Type 1 AGN

G. La Mura

S. Ciroi

V. Cracco

D. Ilić

L. Č. Popović

P. Rafanelli

Department of Astronomy

University of Padua

Dynamical inferences on Super Massive Black Holes from the spectra of broad line emitting Active Galaxies
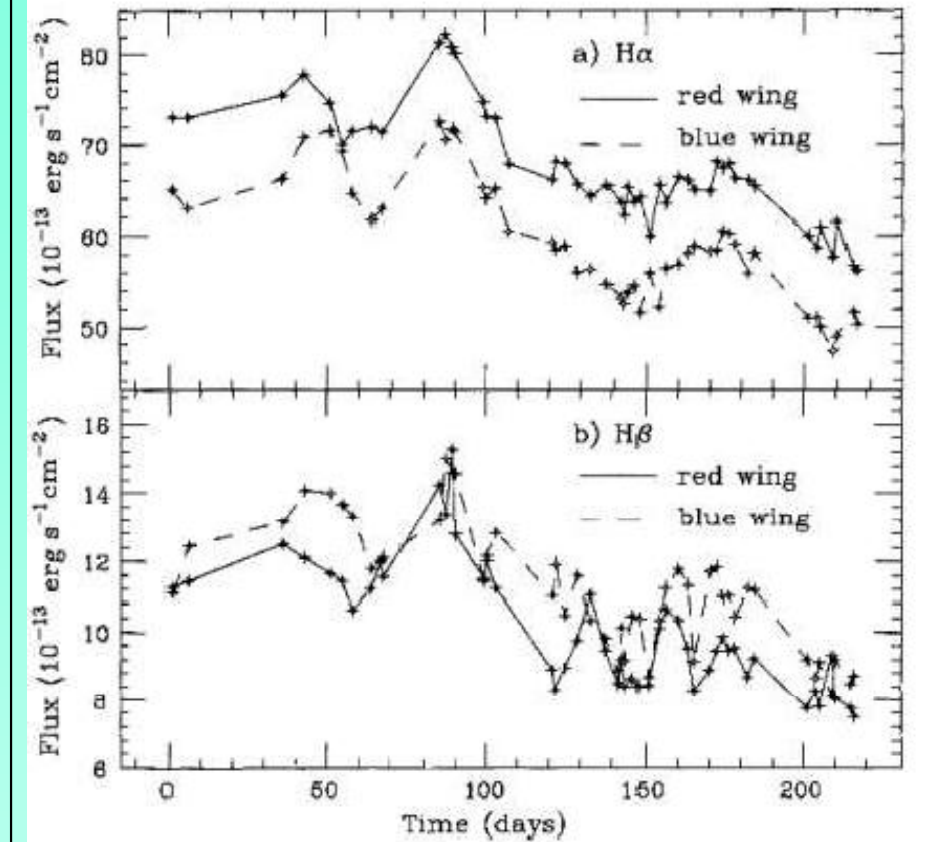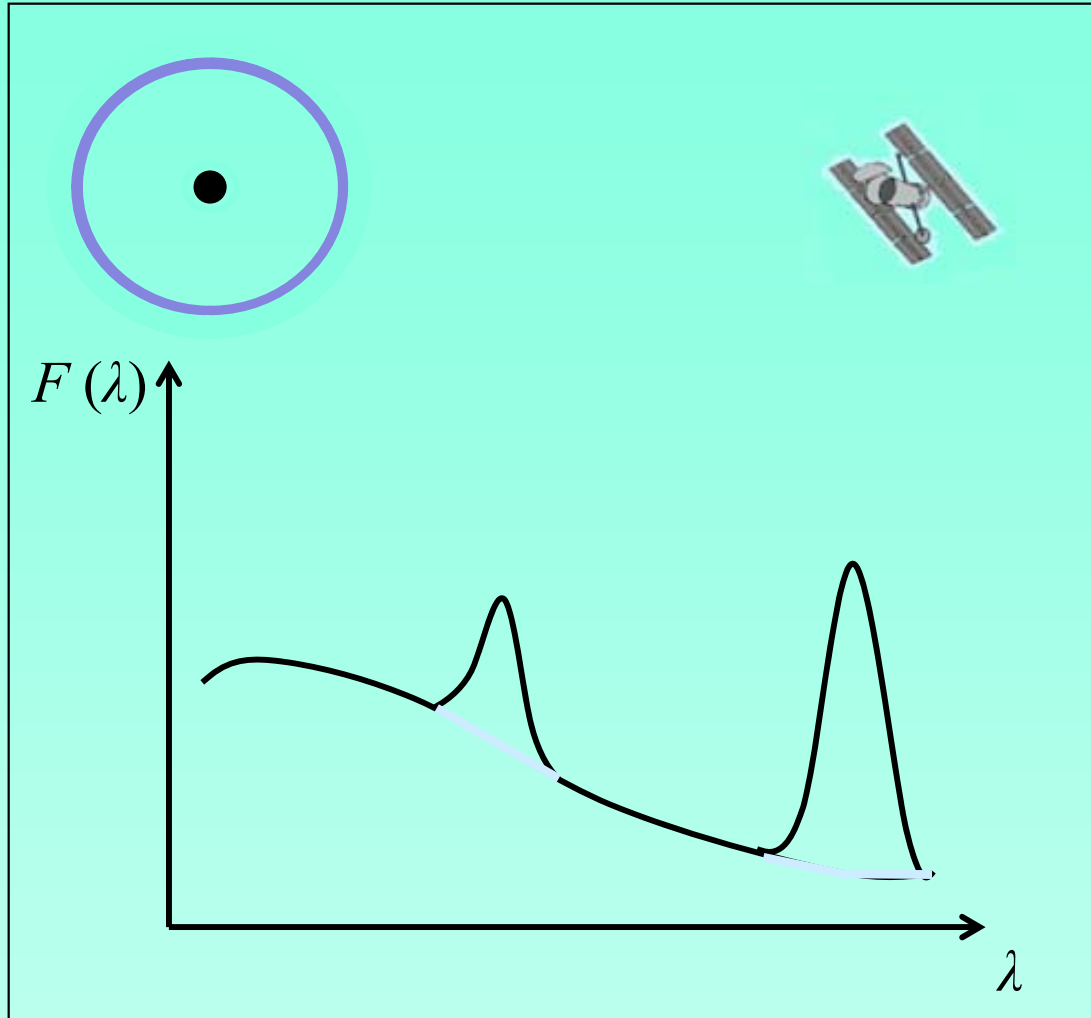
Discussion outline:

1. Physics of the Broad Emission Line Region (BELR)

2. The optical domain: continuum and emission lines

3. Plasma diagnostics with Boltzmann Plots

4. The emission line profiles

5. X-ray observations: analysis and results

6. Concluding remarks

Physics of the BELR
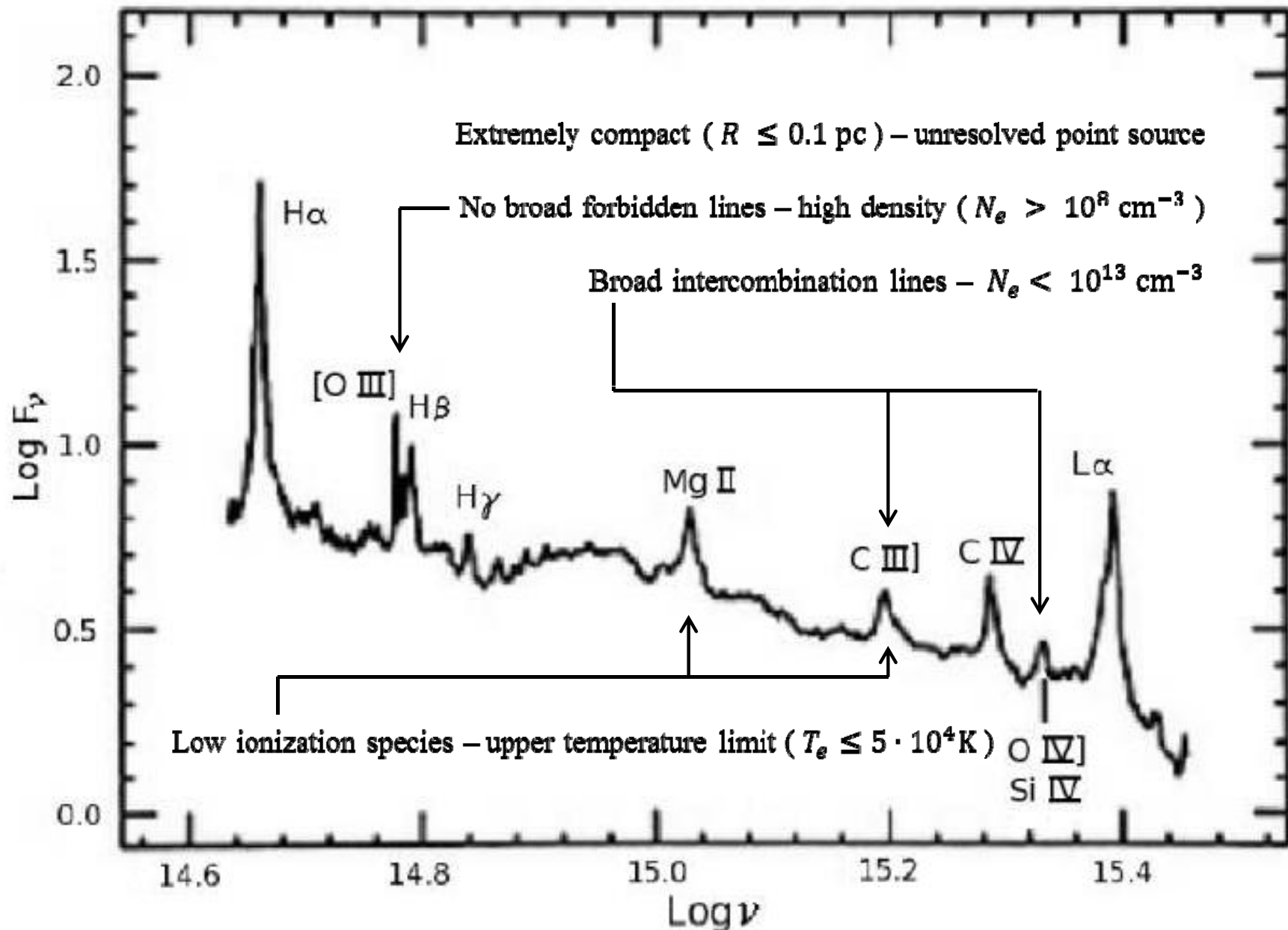
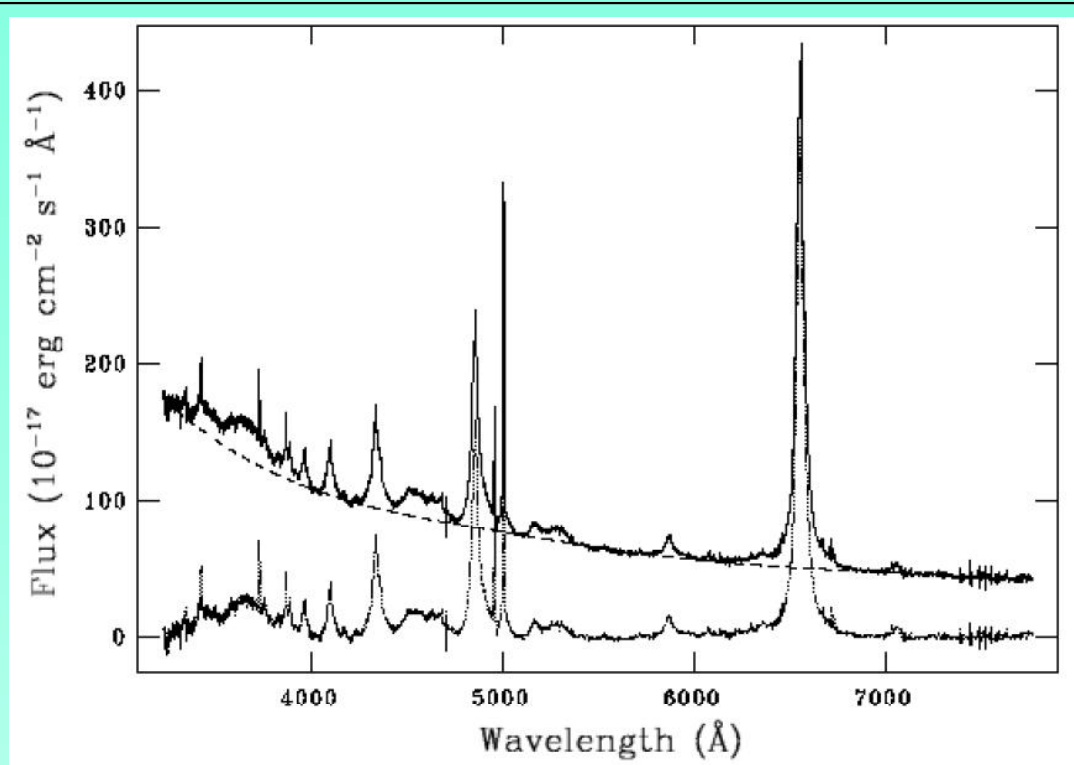A typical Type 1 AGN spectrum (from Netzer 1990)

Physics of the BELR

$F(\lambda)$

λ

a) Hα
— red wing
-- blue wing

b) Hβ
— red wing
-- blue wing

Flux (10^{-13} erg s^{-1} cm^{-2})

Time (days)

Differential emission line light curves in the spectrum of NGC 4151 (Maoz et al. 1991)
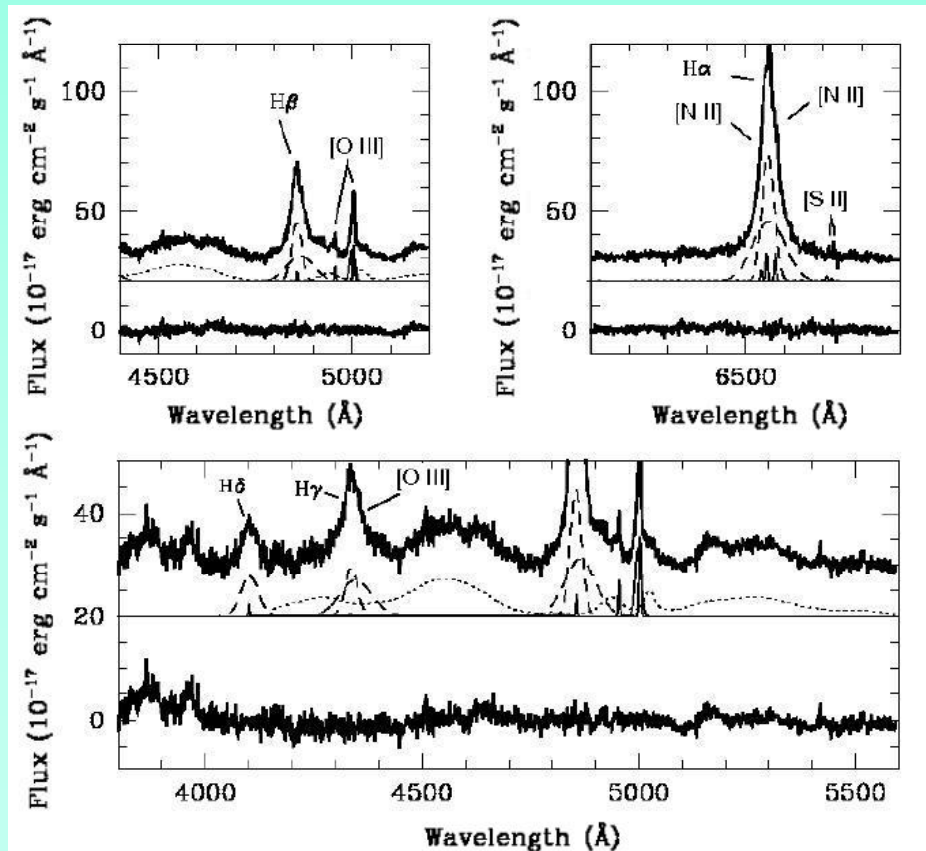
Some details of the BELR structure and kinematics can be derived from the analysis of correlated variations in the continuum and emission lines of the spectra, through the *Reverberation Mapping* (RM) technique.

The optical domain: continuum and emission lines

The identification of the broad spectral line component may be carried out by means of standard techniques, such as the multiple Gaussian profile fits, as it is shown in the case of PC 1014+4717 below.
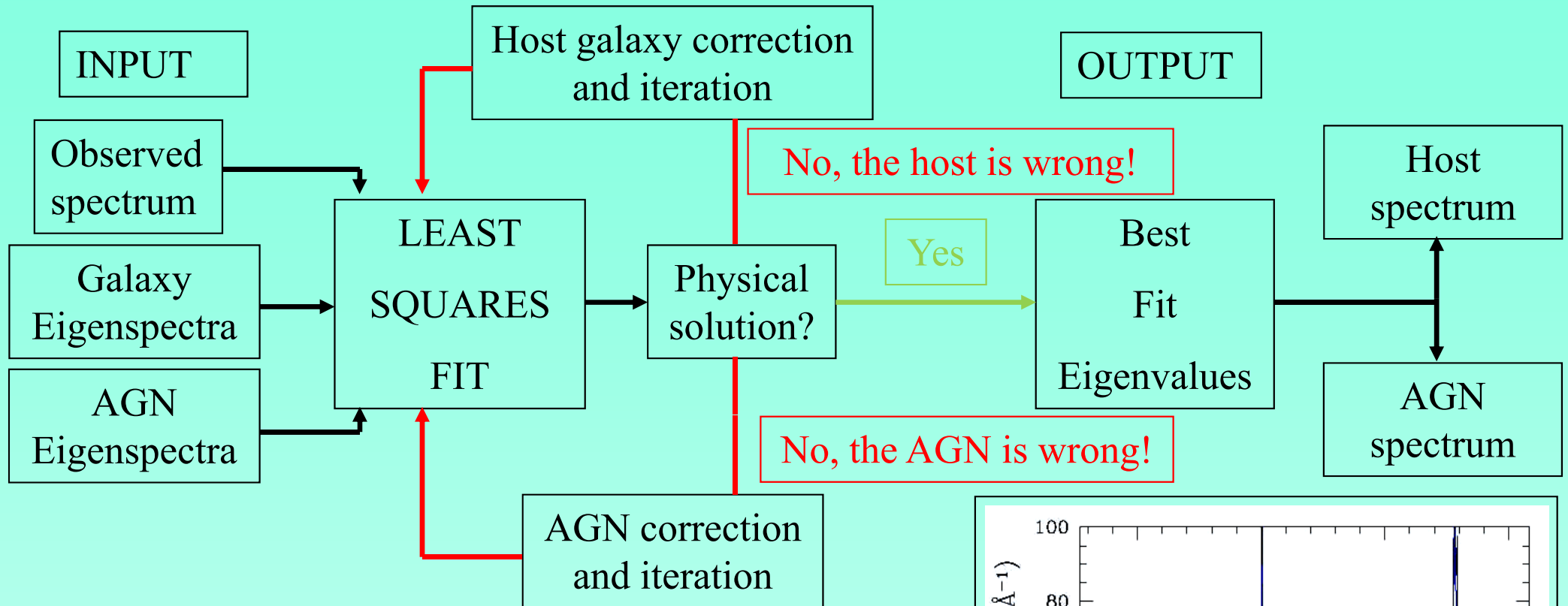

Spectroscopic observations carry several contributions, which are blended together with the BELR signal and must be accounted for, in order to study the broad emission lines. This example illustrates the subtraction of the underlying continuum in the spectrum of 2MASS J03221390+0055134.

The optical domain: continuum and emission lines

INPUT

Host galaxy correction and iteration

OUTPUT

Observed spectrum

Galaxy Eigenspectra

AGN Eigenspectra

LEAST SQUARES FIT

No, the host is wrong!

Physical solution?

Yes

Best Fit Eigenvalues

Host spectrum

AGN spectrum

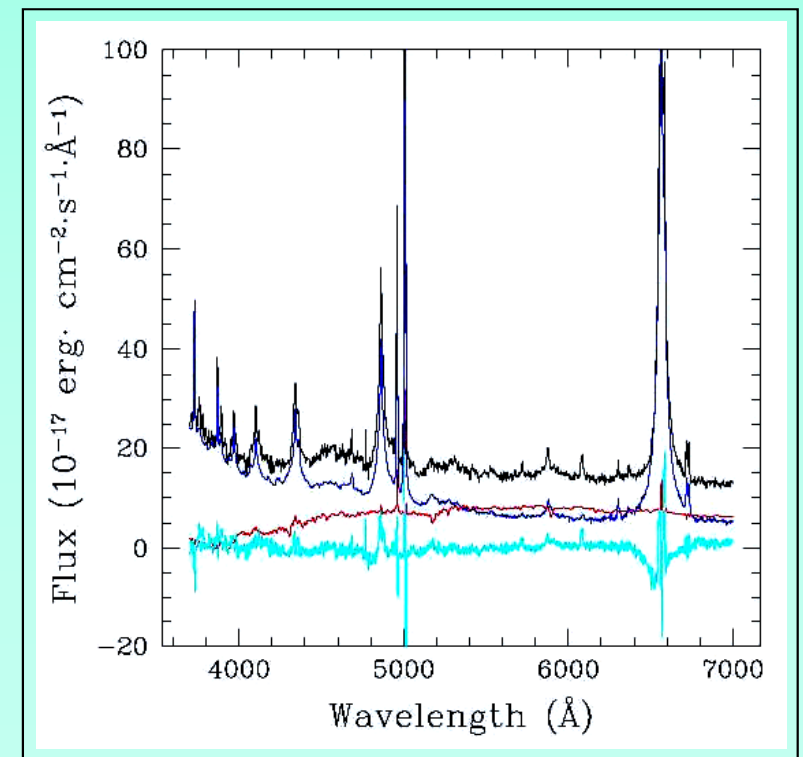No, the AGN is wrong!

AGN correction and iteration

A principal component analysis technique, based on iterative fits to observational data, was developed to isolate the AGN contribution from host galaxy contamination in the SDSS spectra

Connolly et al. 1995, AJ, 110, 1071
Yip et al. 2004, AJ, 128, 585
Yip et al. 2004, AJ, 128, 2603

Plasma diagnostics with Boltzmann Plots

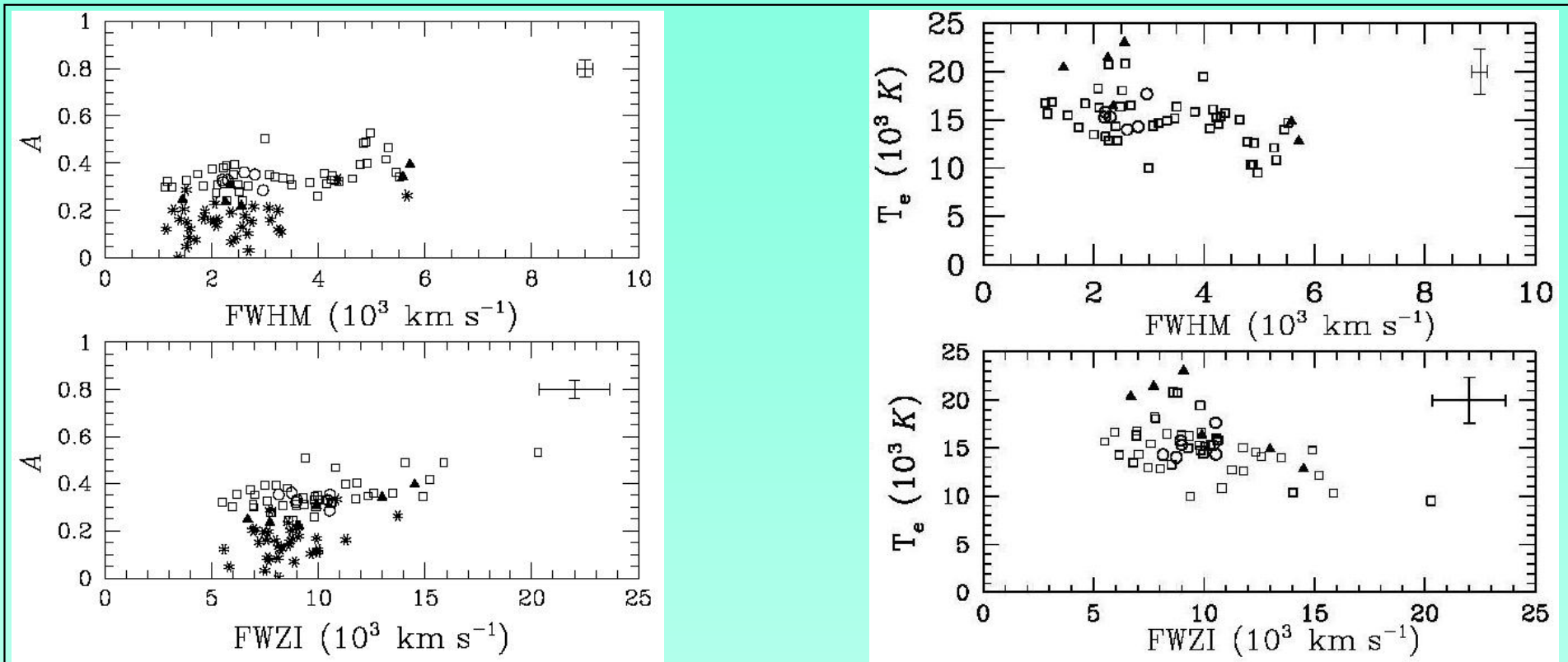**The Boltzmann Plot**: given the normalized line intensity

$$I_n = \frac{\lambda_{ul} F_{ul}}{A_{ul} g_u}.$$

The logarithm of I_n for a particular transition series, in an optically thin plasma, is a linear function of the upper level's excitation energy, with a slope that depends on the plasma electron temperature

$$\log I_n = -\frac{\log e}{k_B T_e} E_u + \text{const.}$$
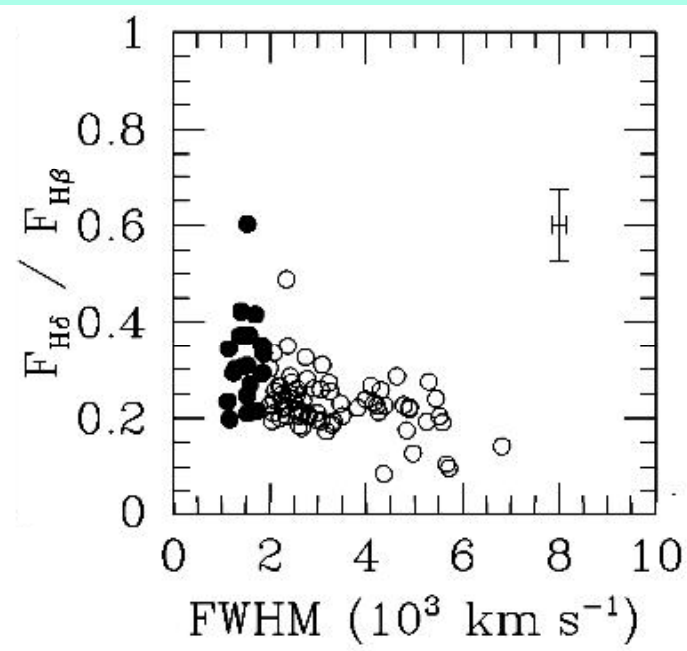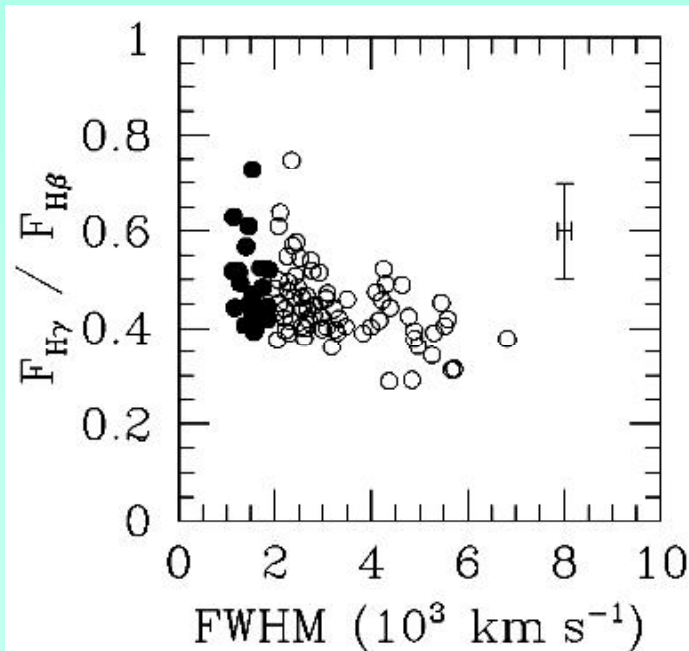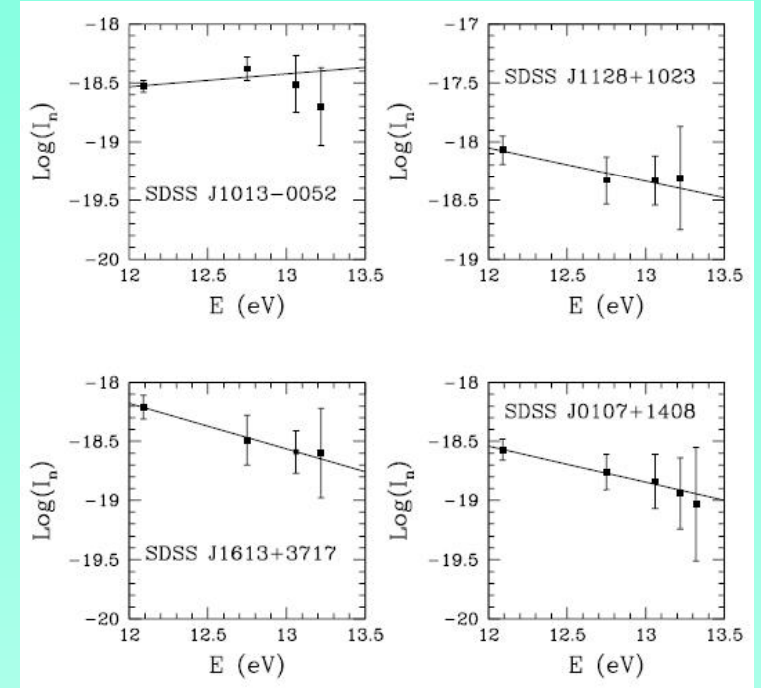
Plasma diagnostics with Boltzmann Plots

Boltzmann Plot slopes as a function of line profile widths (left panel), with the corresponding plasma temperature estimates (right panel).

The Boltzmann Plot assumptions only hold in a fraction of the selected AGN sample (~ 30%), preferably in the range of broad line emitting sources. In narrow lined objects the analysis points towards stronger ionization and higher plasma temperatures (La Mura et al. 2007, ApJ, 671, 104)
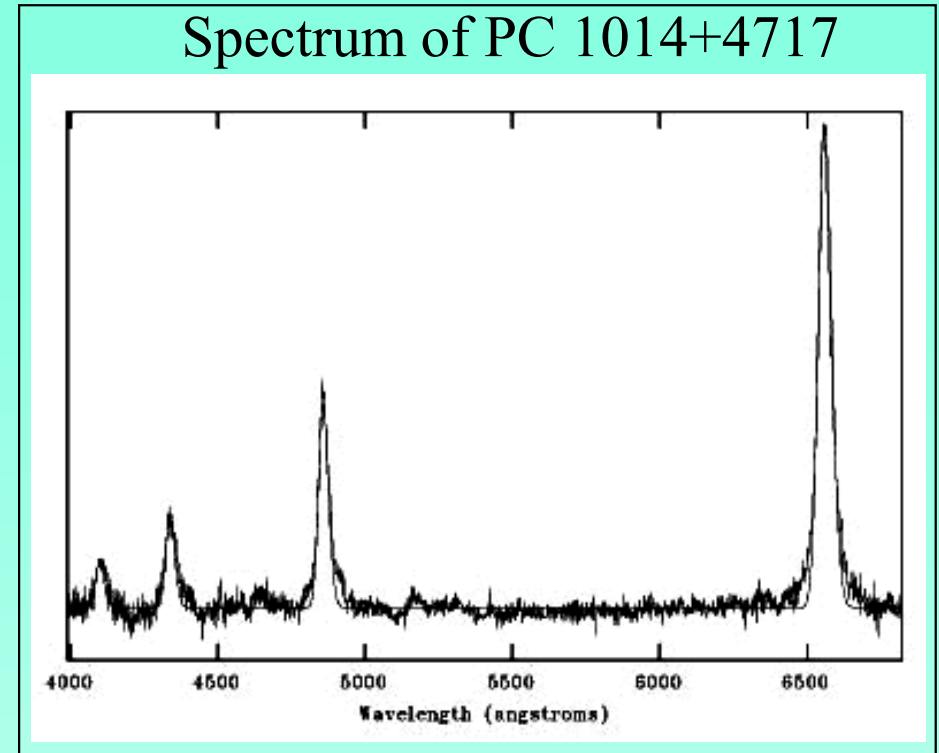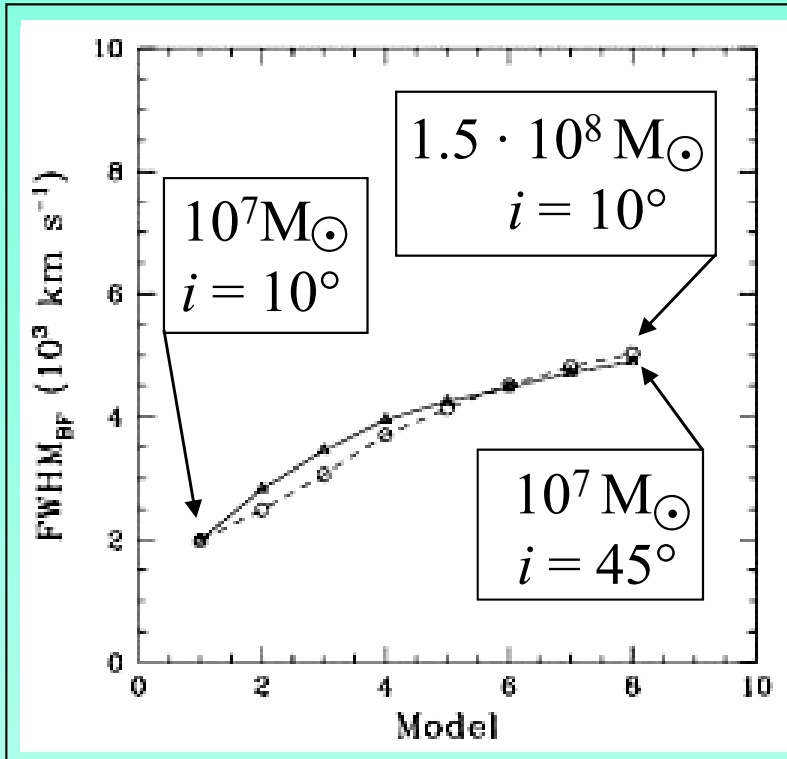
Plasma diagnostics with Boltzmann Plots
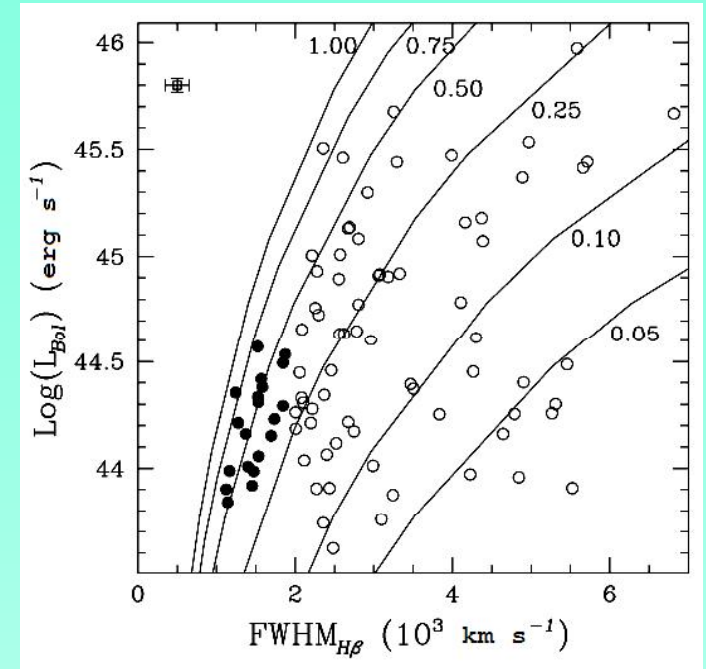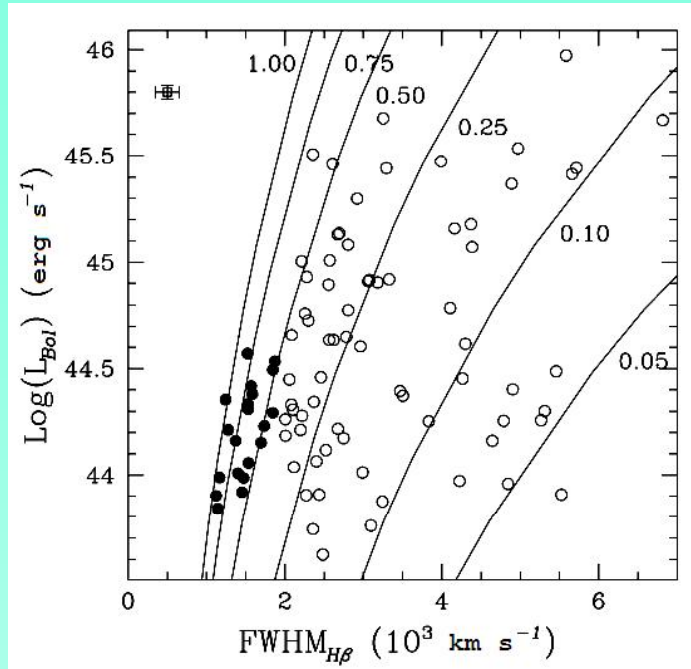
Bolometric luminosities vs. FWHM(Hβ) according to the structural models of Kaspi et al. (left panel) and Bentz et al. (right panel). Filled circles are NLS1 galaxies, while the continuous lines represent SMBH, having masses in the range from $10^6\,M_\odot$ to $10^9\,M_\odot$ and accreting at the labeled Eddington ratios. These observations suggest that objects with narrow emission lines are more commonly powered by low mass black holes working at very high accretion rates.

IT WASN'T SO MASSIVE, AFTER ALL...

The emission line profiles

$10^7 M_{\odot}$
$i = 10°$

$1.5 \cdot 10^8 M_{\odot}$
$i = 10°$

$10^7 M_{\odot}$
$i = 45°$

Spectrum of PC 1014+4717

Given the complex structure of the emission line region, however, the connection among the broad line profiles and the source kinematics is not straightforward. Here we introduce a composite broadening function (BF) based on the Gauss-Hermite polynomial expansion:

$$BF(v) = \frac{B_0}{\sqrt{2\pi}\sigma_v} \exp\left[-\frac{(v - V_{sys})^2}{2\sigma_v^2}\right]\left\{1 + \sum_{i=3}^{N} h_i H_i(v - V_{sys})\right\}$$
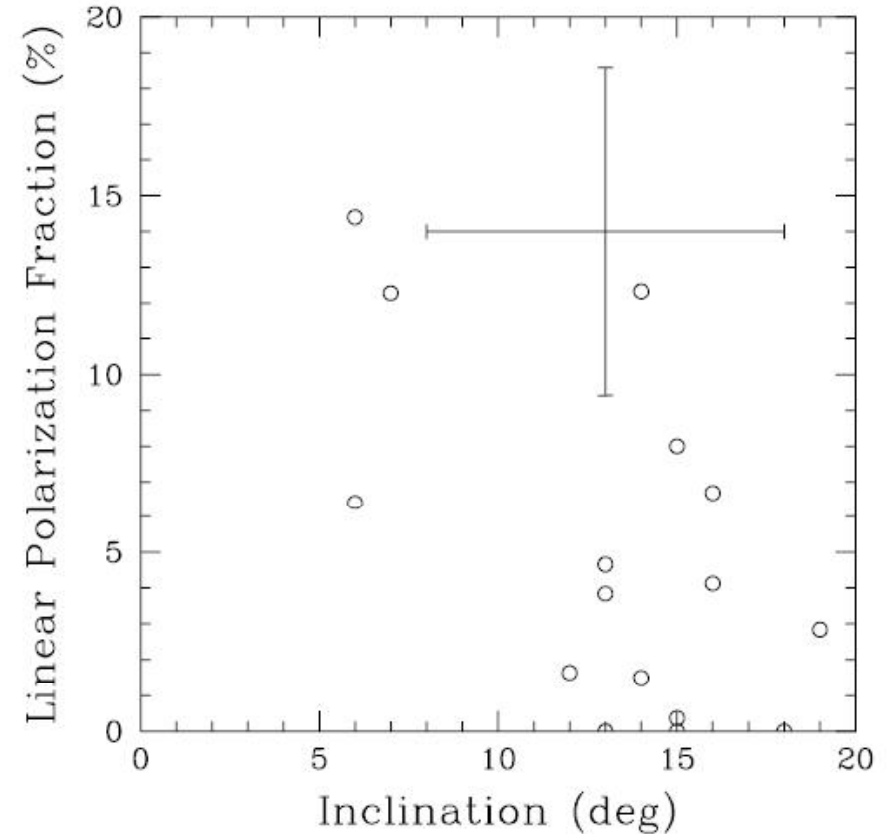
The emission line profiles
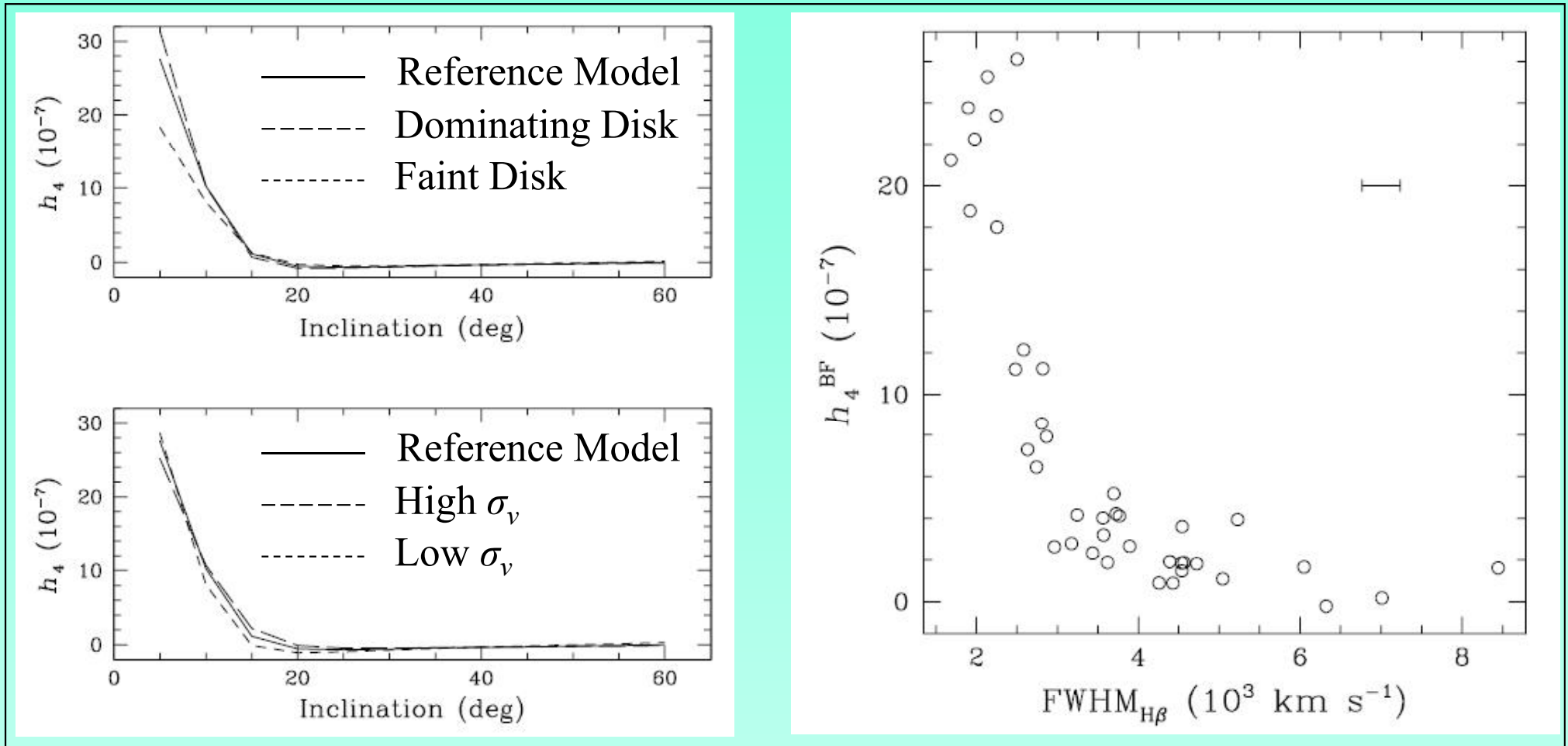
The observed line profile moments are in very good agreement with the predictions of some composite BLR structural models, involving two distinct kinematical contributions: a flat rotating disk, embedded in a surrounding distribution of line emitting material. The inclination of the disk is the main factor affecting the emission line kurtosis.

The emission line profiles
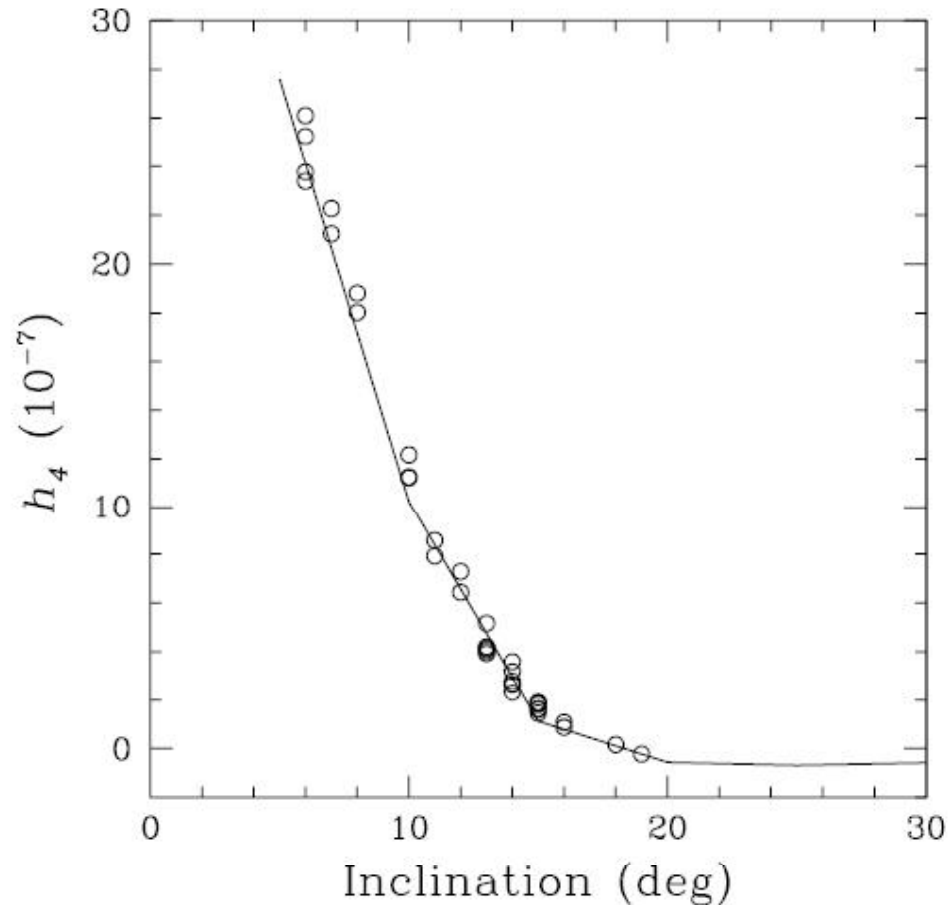
Inclination of BLR, with respect to the line of sight, estimated from the line profile kurtosis predicted by complex BLR structural models, allowing for the existence of a flattened component.

Degree of linear polarization in the radio observations of Type 1 AGN as a function of the inferred BLR inclination with respect to the observational line of sight.
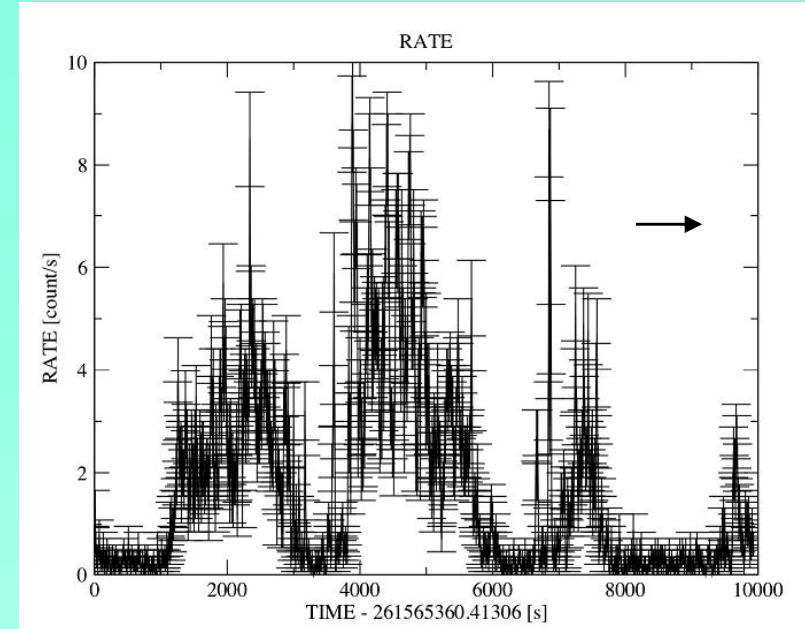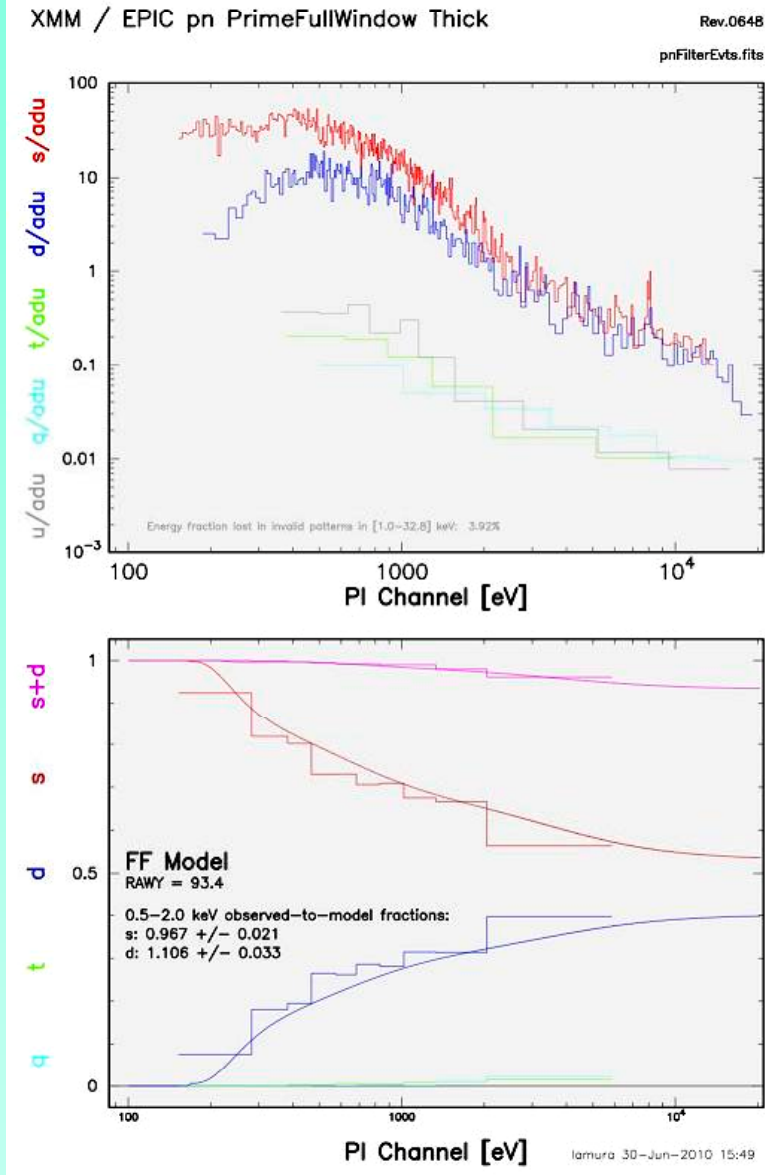
The emission line profiles

$$M_{BH} = f \frac{R_{BLR} v^2}{G} \qquad f \cdot v^2 = v_{eq}^2 = \frac{1}{4}\left[\frac{\sqrt{3}}{2} \mathrm{FWHM}_{Turb} + \frac{\mathrm{FWHM}_{Disk}}{4 \sin i} \right]^2$$
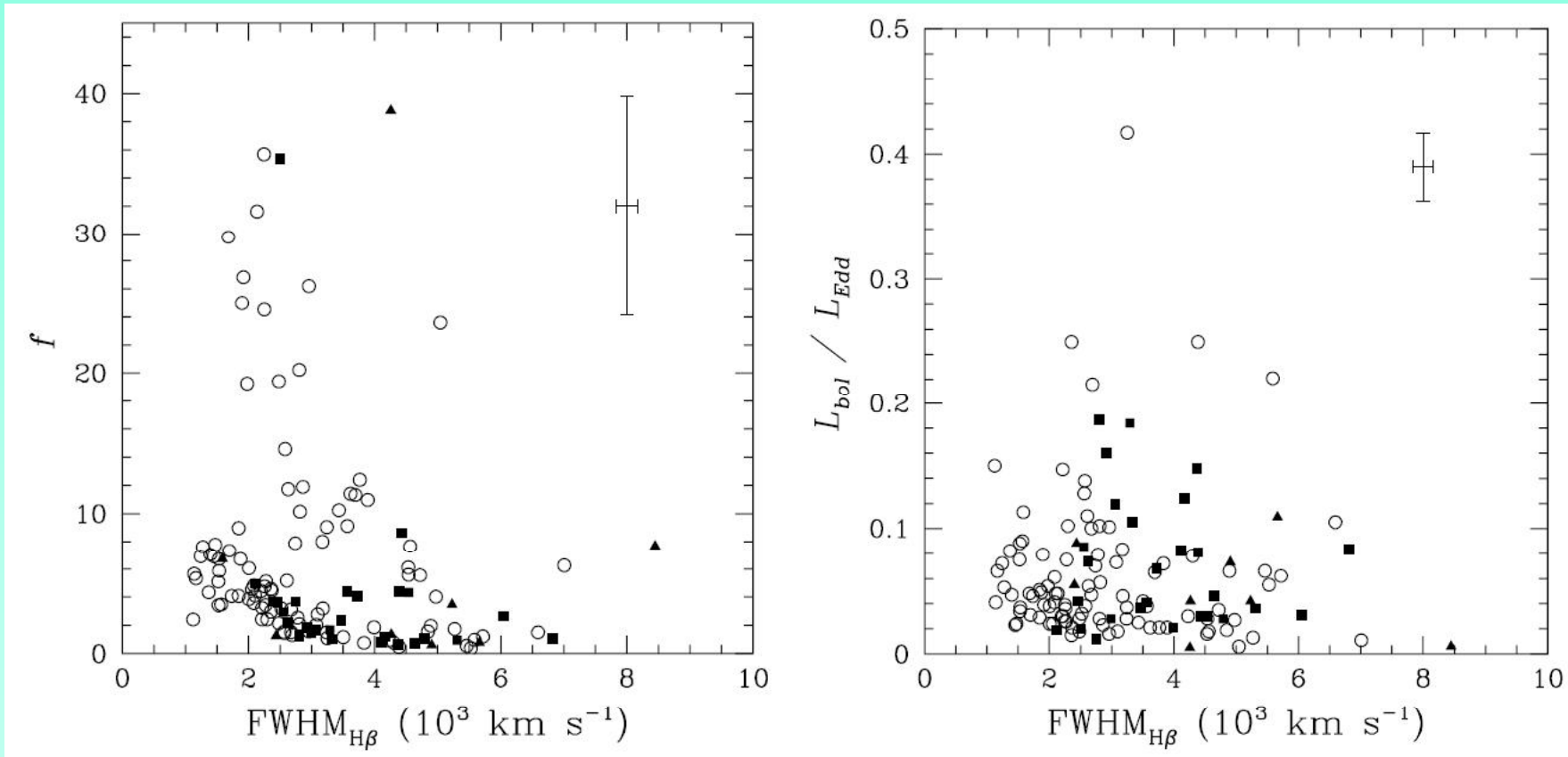

Left: Geometrical factors to estimate the SMBH mass from the profile of Hβ.
Right: Accretion rates onto the SMBH, given in terms of Eddington ratios, as a function of the corresponding FWHM$_{H\beta}$ (from La Mura et al. 2009, ApJ, 693, 1437)
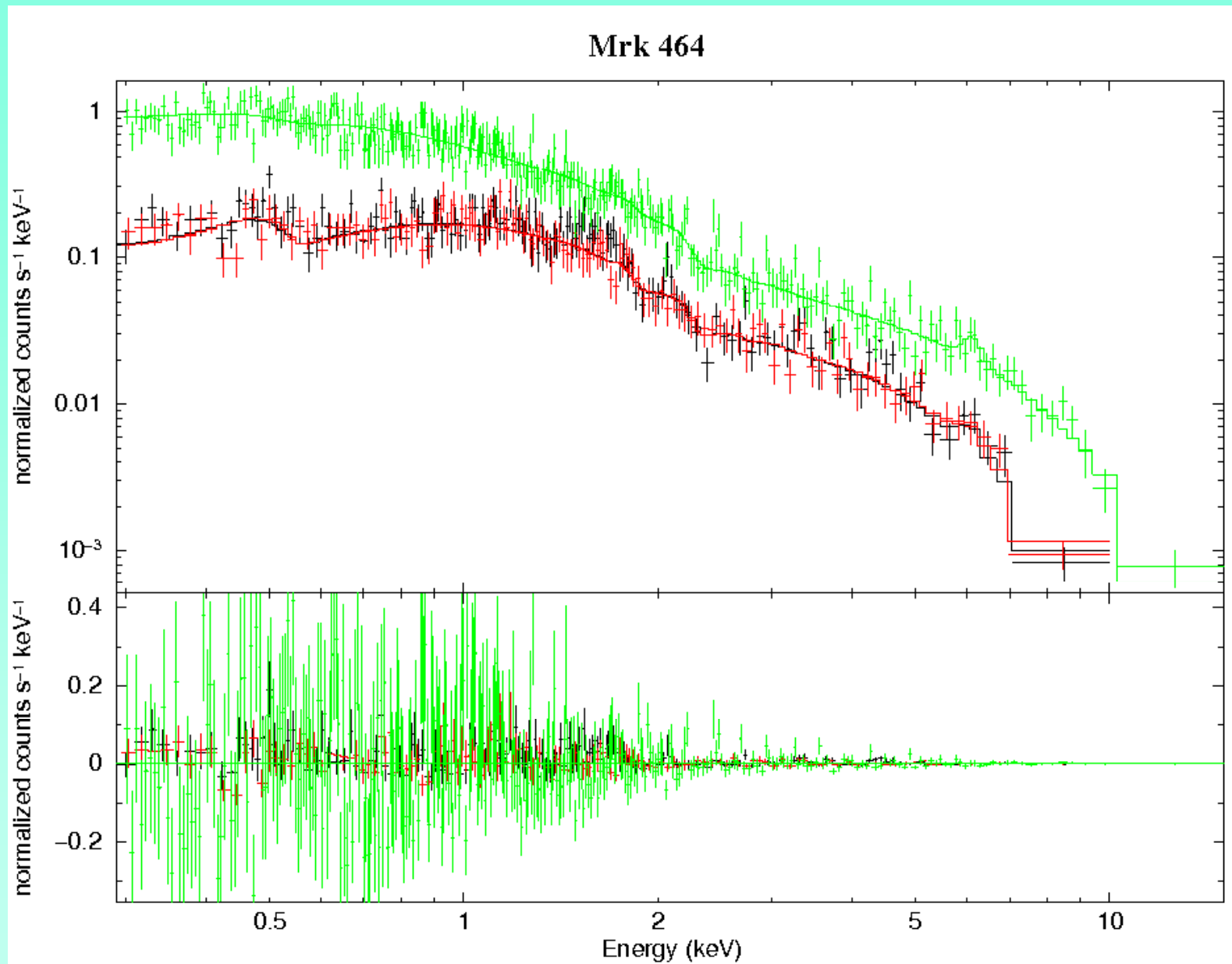
X-ray observations: analysis and results

Flaring particle background can affect the spacecraft, reducing the effective exposure time required for detection of faint objects.
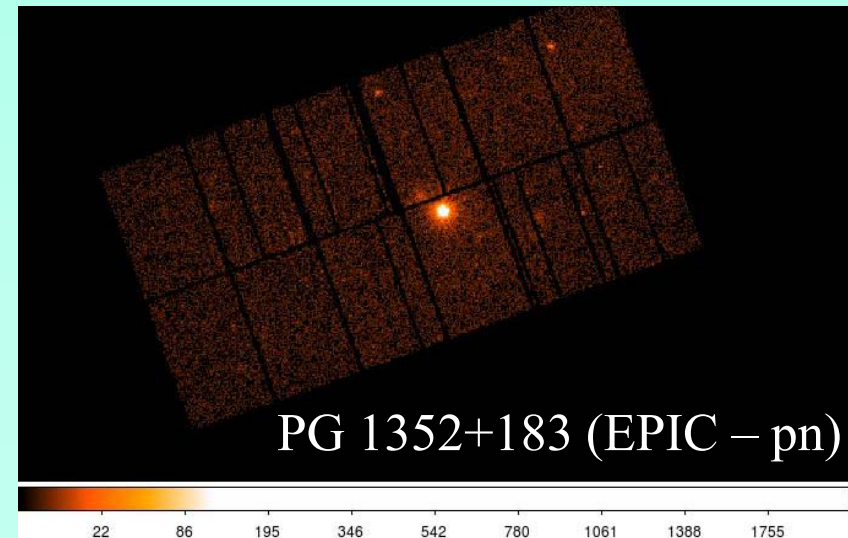
Photon counting pile-up occurs when multiple soft photons are recorded by the detector as a single harder photon.

PG 1352+183 (EPIC – pn)

X-ray observations: analysis and results

Mrk 464

The soft X-ray spectra of BLS1 show a complex thermal component in the soft band, little or no evidence of absorption and a hard X-ray power-law component. A low ionization Fe Kα can usually be detected.

# X-ray observations: analysis and results

MCG +04-22-042
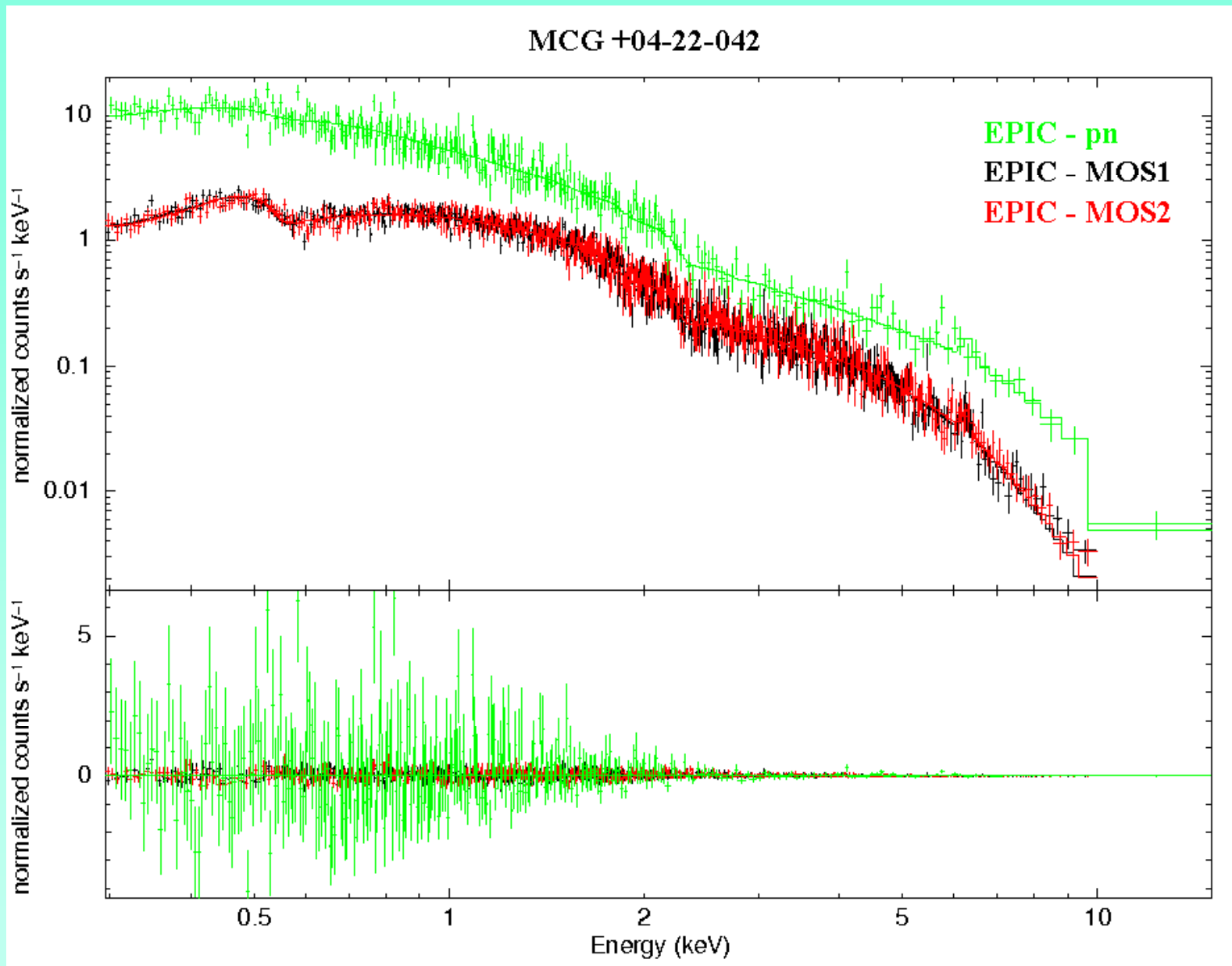
The soft X-ray spectra of NLS1 show a complex thermal component in the soft band, no evidence of absorption and the hard X-ray power-law component. The Fe Kα emission line is detected as the product of reflection by a high ionization medium.

Concluding remarks

Using the FWHM of the Hβ emission line as a flag to investigate the degree of ionization, corresponding to the Fe Kα energy, it is found that the degree of matter ionization increases while moving from the domain of BLS1 galaxies to that of NLS1 objects. Indications for an origin of Fe emission in ionized material have also been pointed out (Romano et al. 2002, ApJ, 564, 162), but a larger sample of observations is still required to assess whether the degree of ionization is actually connected with the optical emission line profiles, as it is suggested by our preliminary results.
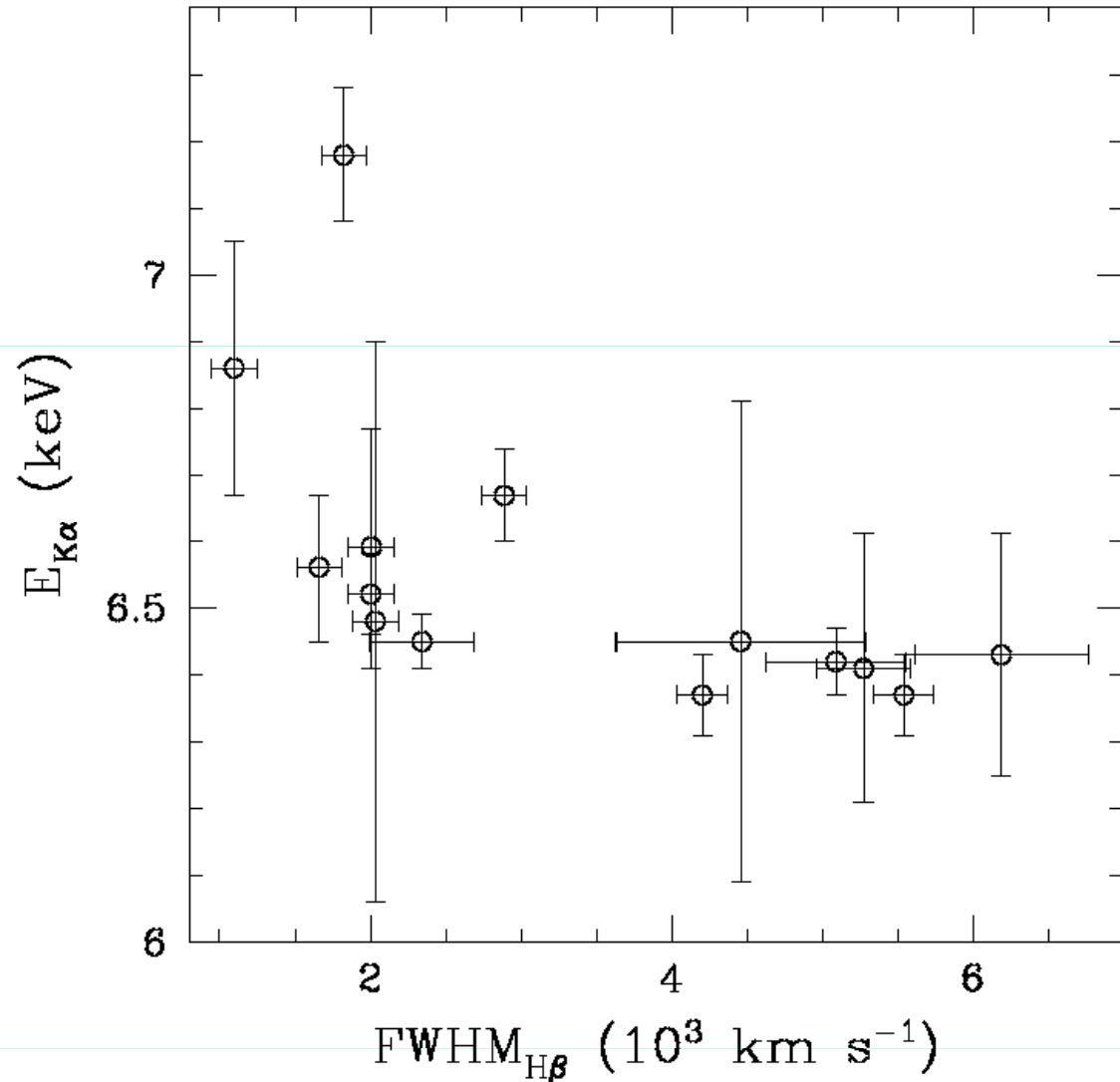
Concluding remarks
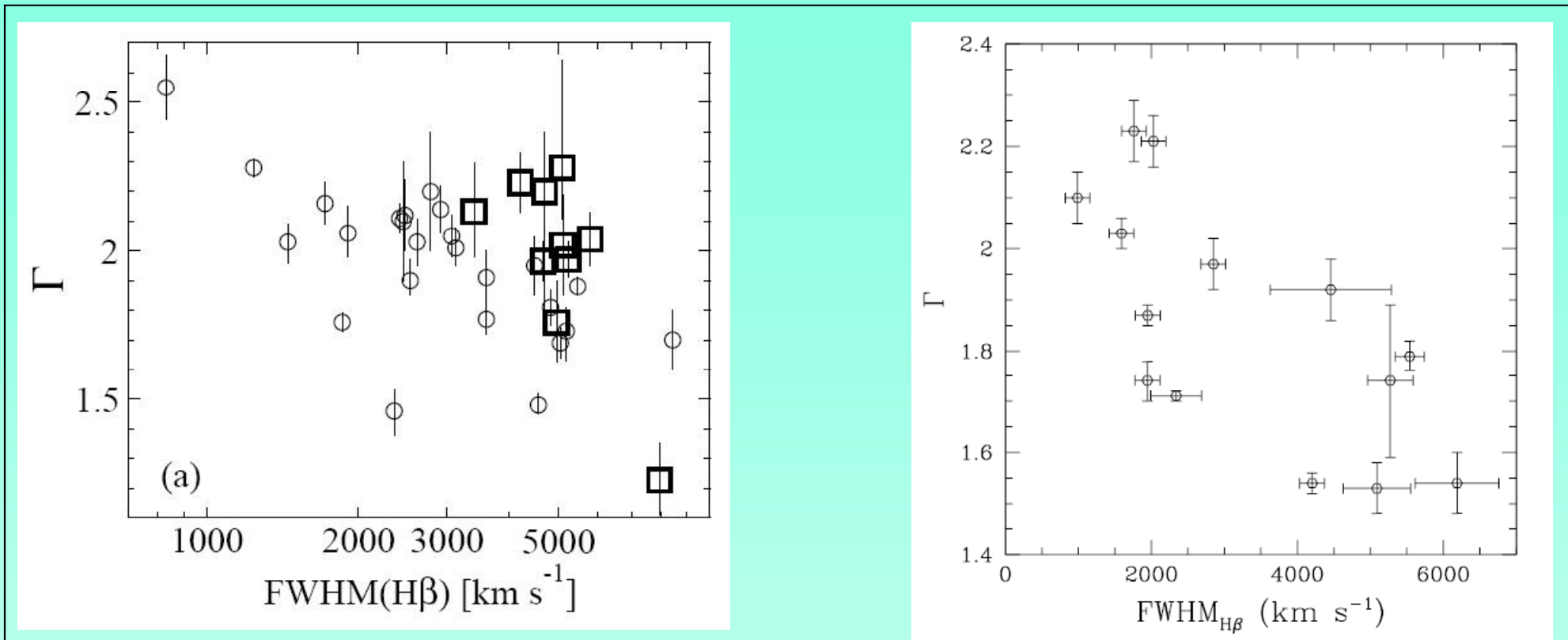
Left: The relationship among the hard X-ray power law slope of low redshift Seyfert1 galaxies (open circles) and high redshift QSO (open squares) and the FWHM of the Hβ emission line (Shemmer et al. 2008, ApJ, 682, 81)
Right: Same relationship plotted as a comparison for the sample of Seyfert 1 galaxies studied in this work.